Raman nanometrology of graphene: Temperature and substrate effects

Irene Calizo [a,*,1], Suchismita Ghosh [a], Wenzhong Bao [b], Feng Miao [b], Chun Ning Lau [b], Alexander A. Balandin [a]

[a] Nano-Device Laboratory, Department of Electrical Engineering, University of California – Riverside, Riverside, CA, USA
[b] Department of Physics and Astronomy, University of California – Riverside, Riverside, CA, USA

ARTICLE INFO

ABSTRACT

Graphene has been a subject of intense interest because of its unique physical properties. Raman spectroscopy became a valuable tool for determining the number of graphene layers and assessing their quality. Here we review our recent results on the effects of substrates and temperatures on Raman signatures of graphene. Specifically, we considered graphene on GaAs, glass, sapphire, standard Si/SiO_2 substrates and suspended across trenches in Si/SiO_2 wafers. We found consistent values for Raman G peak frequency in the suspended graphene and graphene on standard substrates. It was relatively strongly down-shifted by $\sim5\ cm^{-1}$ for graphene on A-plane sapphire. Raman inspection of many spots on graphene layers on glass indicated that in some instances G peak was split into doublets. We investigated the temperature dependence of the Raman spectrum of graphene and found that G peak red shifts with increasing temperature despite graphene's negative coefficient of thermal expansion. Using the measured temperature coefficient of graphene G peak we were able to adopt Raman spectroscopy for determining the thermal conductivity of graphene. The knowledge of the temperature and substrate effects on graphene Raman spectra is important for extending the application of micro-Raman spectroscopy as a nanometrology tool for graphene characterization and graphene device fabrication.

1. Introduction

Graphene generated a lot of interest owing to its exotic physical properties and proposed applications in field-effect transistors, high-speed analog electronics, ultra sensitive chemical detectors, interconnects and spintronic devices [1–9]. One of the major hurdles in graphene research is the difficulty of accurately counting the number of atomic layers in samples obtained by either mechanical exfoliation from bulk graphite or grown by some other means. The ability to see graphene on Si/SiO_2 substrates with a certain thickness of oxide layer in an optical microscope was instrumental in the initial boom in graphene research. At the same time, optical inspection has proven to be a rather difficult – if not impossible – technique to definitively identify the number of layers of graphene. Typically single and bilayer graphene flakes are outnumbered by much thicker graphene flakes which make the search for graphene a formidable task. Atomic force microscopy (AFM) alone may not clearly identify the number of graphene layers. Other alternatives include low-temperature transport studies or cross-sectional transmission electron microscopy (TEM). The major disadvantages of these methods include lengthy and involved experimental or sample preparation procedures.

Recently micro-Raman spectroscopy has become a conventional technique for the identification and characterization of graphene layers [10–13]. It is a fast, nondestructive, high-throughput and unambiguous approach. The Raman spectrum of graphene is very sensitive to the number of atomic layers and the presence of disorder or defects, which allows for accurate graphene characterization. Most Raman spectroscopic studies of graphene have been carried out for graphene on standard Si/SiO_2 substrates with 300 nm thickness of the oxide layer. These substrates ensured graphene visibility under optical microscopes [14]. In order to extend the use of Raman spectroscopy as a graphene nanometrology tool, one needs to study how the Raman signatures of graphene are affected when graphene is placed on substrates made of different materials, as well as investigate the effect of temperature.

In this paper we review our results and present some new data for Raman microscopy of graphene on n-type (100) GaAs, glass, and A-plane ($11\bar{2}0$) sapphire substrates. We also outline the temperature dependent Raman scattering studies of single and bilayer graphene on Si/SiO_2 substrates. In addition, the application of Raman spectroscopy for the measurements of the thermal conductivity is briefly discussed.

---

* Corresponding author.
  E-mail address: icalizo@ee.ucr.edu (I. Calizo).
1 Present address: National Institute of Standards and Technology, Gaithersburg, MD, USA.
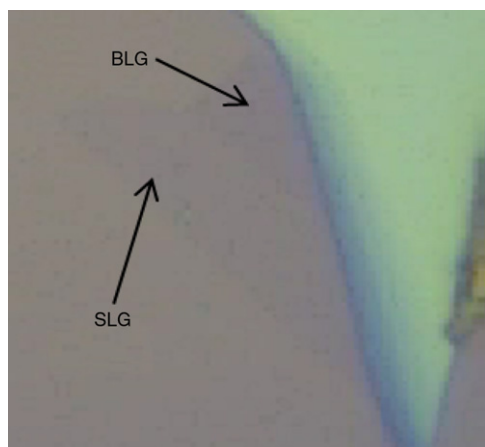
Fig. 1. Optical image of single and bilayer graphene on Si/SiO$_2$ used for Raman studies.

Fig. 2. Raman spectrum of graphene on a Si/SiO$_2$ substrate around 2D band region. Note the changes in the spectra as the number of layers, n, increases from 1 to 5.

2. Materials and methods

Graphene samples used in this work were prepared by micromechanical cleavage of bulk Kish graphite and highly oriented pyrolitic graphite (HOPG). The samples used for the measurement of thermal conductivity were suspended over a trench made through the 300 nm oxide on the Si/SiO$_2$ substrate. Raman spectra were collected from a Renishaw Raman spectrometer in a backscattering configuration. The microscope was fitted with a 50x objective lens (NA = 0.75). All measurements reported here were carried out with a 488 nm visible excitation laser source with laser powers below 4.8 mW. The latter was to avoid any local heating in the samples. In the case of the thermal conductivity measurements, the power was intentionally increased to see the changes in the Raman G peak due to the local temperature variation. Measurements were performed at several locations across the flakes to ensure that the changes in peak position were not from spatial variations.

In our temperature dependent Raman measurements, the graphene samples were placed in a liquid-nitrogen pumped hot-cold cell. The sample temperature was increased from −160 °C to 100 °C in 10 °C intervals with an accuracy of ±0.1 °C. Fig. 1 shows an image of the sample taken from an optical microscope. Single layer graphene appears a very light, almost invisible, purple color while bilayer graphene flakes are a slightly darker purple under the microscope. As the number of graphene layers increase, the flake becomes bluer. AFM confirmed the number of layers and quality of the graphene flakes. The 2D-peak deconvolution was performed using Renishaw's WiRE software.

3. Substrate effects

Since graphene is just a single atomic layer of carbon, it is unclear how strong the effects of the substrate and surface contamination on Raman spectra are. It is not obvious that the main Raman features used for graphene identification will remain the same when graphene is transferred to substrates other than Si/SiO$_2$. The G peak of graphene, which appears at about 1580 cm^{-1}, represents the E_{2g} in-plane vibrational modes. A disorder D band appears at about 1350 cm^{-1} in the presence of defects and close to the edge of the flake. The D-band corresponds to the in-plane A_{1g} (LA) zone-edge mode [15]. In most of the examined samples the D-band was not visible, which confirmed the high quality of the samples.

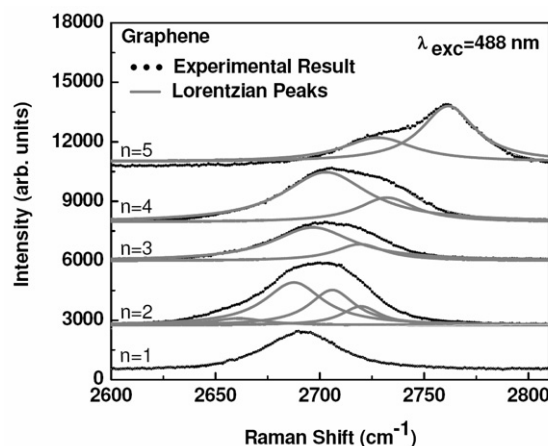Based on our experience of handling many graphene samples, the most informative part of Raman spectrum of graphene is 2D
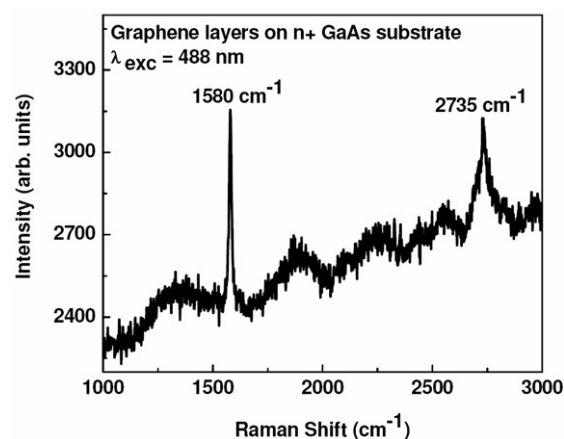

Fig. 3. Raman spectrum of graphene layers on $n+$ GaAs.

band region (see Fig. 2). The position and the shape of the 2D band, occurring at about 2700 cm^{-1}, have been explained by the double-resonance model [11,16]. Fig. 2 shows the evolution of the 2D band as the number of layers increases from single to 5-layered graphene. The evolution of 2D band, position of G peak and relative intensity of G and 2D bands have been used for determining the number of layers. The number of layers was also checked with AFM and, for some samples, with transport measurements [13]. The Raman spectrum of graphene on GaAs is seen in Fig. 3. The typical spectra of graphene-on-GaAs are much noisier than those of graphene on standard substrates. At the same time, one can always find typical features such that G peak at ∼1580 cm^{-1} and 2D band, occurring here at 2736 cm^{-1}. The 2D band deconvolution can still be used for determining the number of atomic layers. For example, the spectrum in Fig. 3 corresponds to the flake with five atomic layers.

Some substrates produced stronger effects on graphene Raman signatures. In Fig. 4 the G peak position is red-shifted by ∼5 cm^{-1}. The shift was observed consistently in many locations on the sample surface. This effect, which was not observed for other substrates, may be related to a stronger interaction between graphene and A-plane sapphire substrates. A similar effect was reported for carbon nanotubes on A-plane sapphire [17]. Fig. 5(a) shows the Raman spectrum of graphene layers on glass. Its peak position remains in its expected position. However, in some instances, the peak splits. Random defects or charges on the surface may explain the doublets [13]. Fig. 5(b) is the 2D band of bilayer graphene on a glass substrate. The same four elemental
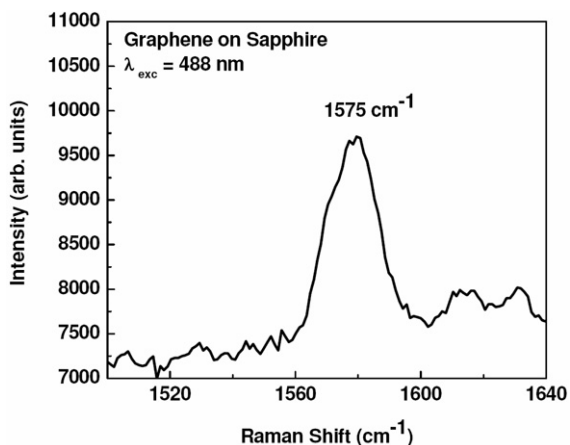
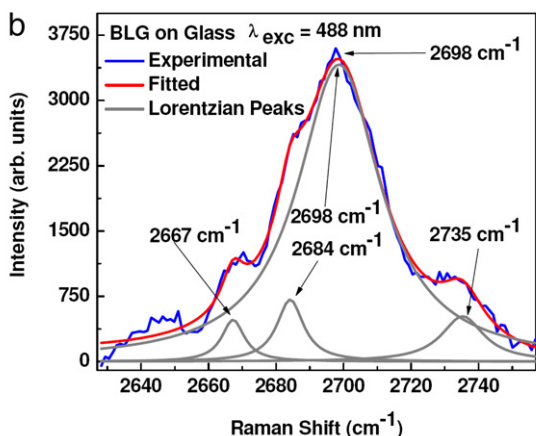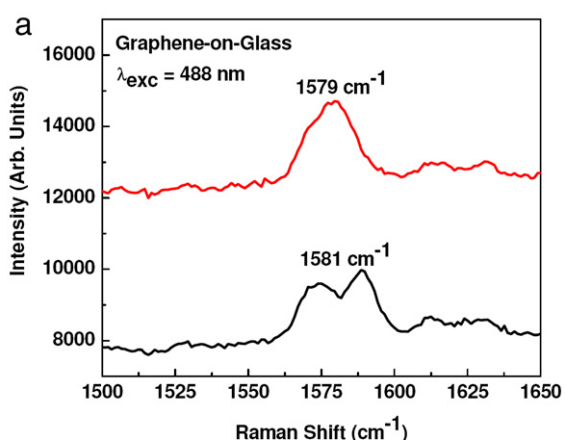**Fig. 4.** Raman *G* peak of graphene-on-sapphire.

Fig. 5. (a) Raman spectrum of graphene layers on glass; (b) Raman peak deconvolution of bilayer graphene on glass substrate.

peaks, as predicted by the double resonance Raman model, can be distinguished in the Raman spectrum of bilayer graphene on the glass substrate. Based on these studies, our conclusion was that the 2*D* band deconvolution method of counting the number of graphene layers was applicable to the substrates made of different materials, including amorphous glass substrates with a large number of defects.

4. Raman *G* peak temperature dependence

It is important to separate the effects due to temperature from those due to the change in the number of graphene
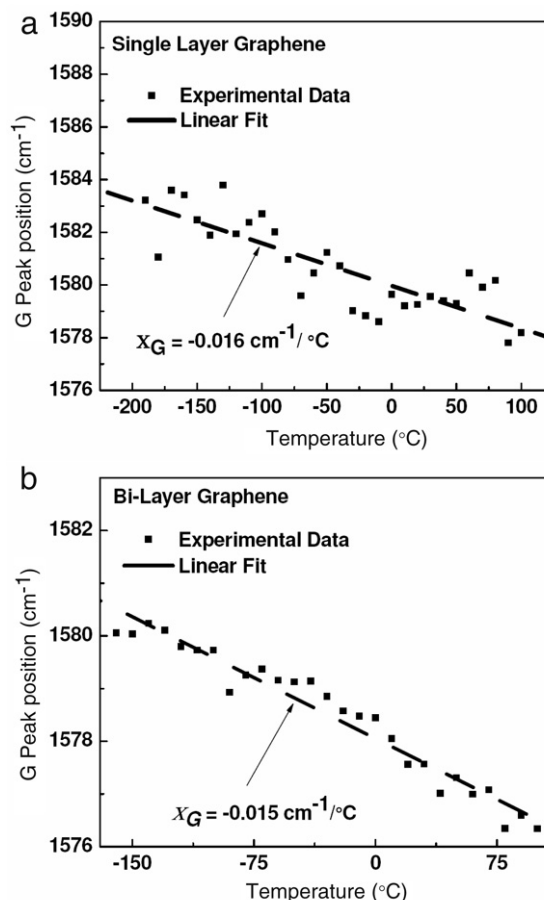

Fig. 6. Temperature coefficients for the Raman *G* peak of (a) single layer graphene and (b) bilayer graphene.

layers. Variations in temperature can result from local laser heating or application of gate and bias voltages. The temperature coefficients of graphene can provide important information on the inharmonicity of graphene crystal lattice. We also used temperature coefficients for the measurement of the thermal conductivity of graphene. Fig. 6 shows the temperature dependence of the Raman *G* peak position for single and bilayer graphene. The slope of the linear fit gives the value of the temperature coefficient, χ_G, which is defined through the expression $\omega = \omega_0 + \chi T$ where ω_G^0 is the frequency of the *G* peak extrapolated to 0 K. The *G* peak temperature coefficient for bilayer and single layer graphene is $\chi_{G,BLG} = -0.015$ cm^{-1}/K and $\chi_{G,SLG} = -0.016$ cm^{-1}/K, respectively. As temperature increases, the *G* peak position shifts to lower wave numbers, leading to a red shift. Knowing this coefficient, one can essentially use a Raman spectrometer as a thermometer, with the position of the Raman *G* peak determining the current temperature. We also measured the temperature coefficient for highly oriented pyrolitic graphite (HOPG), which was used as a reference. Our results are in excellent agreement with the data reported for HOPG earlier [18].

The Raman spectrum of the *G* peak of single layer graphene is shown in Fig. 7 at 100 °C and 160 °C. The red shift with increasing temperature is clearly visible [19]. The full width at half maximum (FWHM) for single layer graphene and bilayer graphene at room temperature was 13.5 cm^{-1} and 18.2 cm^{-1} respectively. The red shift of the *G* peak with temperature may appear unusual due to the fact that graphene has a negative coefficient of thermal expansion. The ab initio calculations of the in-plane coefficient of linear expansion predicted a negative value up to 2300 K [20]. This means that as the temperature increases
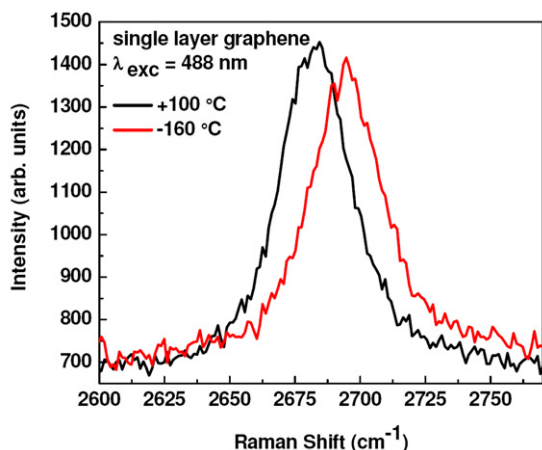
Fig. 7. *G* peak Raman spectrum of single layer graphene at 100 °C and −160°C.
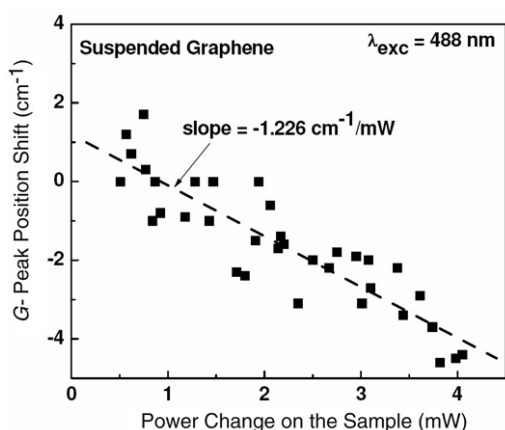

Fig. 8. Shift of Raman *G* peak with the excitation laser power.

the bond length decreases and graphene experiences thermal contraction instead of expansion. Materials, which experience a decrease in the bond–bond length, usually reveal a blue-shift of the characteristic Raman peaks. Our experimental findings were explained by a recent theoretical work [21], which has shown that despite the bond–bond length decrease with temperature, the overall crystal behavior is dominated by the four-phonon interaction resulting in *G* peak red shift.

The micro-Raman nanometrology was successfully used for characterization and quality control of graphene produced by the high pressure – high temperature (HPHT) growth process [22]. The new method of graphene synthesis uses natural graphitic source materials and molten Fe–Ni catalysts for dissolution of carbon. The carbon is then re-crystallized with the help of a seed crystal. The resulting large-area graphene flakes were selected with the help of spectroscopic micro-Raman and scanning electron microscopy. The disorder-induced *D*-peak ∼1359 cm^{-1}, while very strong in the initial graphitic material, was absent from the graphene layers.

5. Thermal conductivity of Graphene

By measuring both the Raman *G* peak temperature coefficients and dependence of the *G* peak position on laser power (Fig. 8), we were able to extract the thermal conductivity of suspended graphene [23,24]. Due to the extremely small thickness of graphene flake, a very low laser power absorbed in the flake produced a measurable temperature rise. The amount of laser

power dissipated in graphene was determined through the original calibration procedure developed by us, by comparing the integrated Raman intensity of *G* peak from graphene and HOPG. Using this Raman-based method, we determined that the thermal conductivity of single layer graphene measured at room temperature is in excess of 3080 W/mK. The latter means that the thermal conductivity of graphene is on the upper end of the values reported for carbon nanotubes or exceeds them. The superior heat conduction properties of graphene combined with its flat geometry make graphene a promising material for thermal management of nanoelectronic circuits and interconnect applications [25,26].

6. Conclusions

Micro-Raman spectroscopy is an invaluable nanometrology tool for graphene and graphene devices, which can be applied to graphene on various substrates. The Raman spectral features give sufficient information to determine the number of atomic layers and assess the quality of the graphene materials. The determined temperature coefficients for graphene *G* and 2*D* bands allow one to take into account the external temperature variations or local laser heating during the Raman inspection. The Raman spectroscopy was successfully used to measure the thermal conductivity of suspended graphene via a non-contact optical technique.

References

[1] A.K. Geim, K.S. Novoselov, Nature 6 (2007) 183.
[2] E.V. Castro, K.S. Novoselov, S.V. Morozov, N.M.R. Peres, J.M.B. Lopes dos Santos, J Nilsson, F. Guinea, A.K. Geim, A.H. Castro Neto, Phys. Rev. Lett. 99 (2007) 216802.
[3] K.S. Novoselov, A.K. Geim, S.V. Morozov, D. Jiang, Y. Zhang, S.V. Dubonos, I.V. Grigorieva, A.A. Firsov, Science 306 (2004) 666.
[4] F. Miao, S. Wijeratne, Y. Zhang, U.C. Coskun, W. Bao, C.N. Lau, Science 317 (2007) 1530.
[5] F. Schedin, A.K. Geim, S.V. Morozov, E.W. Hill, P. Blake, M.I. Katsnelson, K.S. Novoselov, Nature Mater. 6 (2007) 652.
[6] O. Yazyev, M.I. Katsnelson, Phys. Rev. Lett. 100 (2008) 047209.
[7] X. Wang, Y. Ouyang, H. Wang, J. Guo, H. Dai, Phys. Rev. Lett. 100 (2008) 206803.
[8] J-H. Chen, C. Jang, S. Xiao, M. Ishigami, M.S. Fuhrer, Nature Nano. 3 (2008) 206.
[9] K.S. Vovoselov, E. McCann, S.V. Morozov, V.I. Fal'ko, M.I. Katsnelson, U. Zeitler, D. Jiang, F. Schedin, A.K. Geim, Nature Phys. 2 (2006) 177.
[10] A.C. Ferrari, J.C. Meyer, V. Scardaci, C. Casiraghi, M. Lazzeri, F. Mauri, S. Piscanec, D. Jiang, K.S. Novoselov, S. Roth, A.K. Geim, Phys. Rev. Lett. 97 (2006) 187401.
[11] A. Gupta, G. Chen, P. Joshi, S. Takigadapa, P.C. Eklund, Nano Lett. 6 (2006) 2667.
[12] I. Calizo, W. Bao, F. Miao, C.N. Lau, A.A. Balandin, Appl. Phys. Lett. 91 (2007) 201904;
I. Calizo, D. Teweldebrhan, W. Bao, F. Miao, C.N. Lau, A.A. Balandin, J. Phys. C 109 (2008) 012008.
[13] I. Calizo, F. Miao, W. Bao, C.N. Lau, A.A. Balandin, Appl. Phys. Lett. 91 (2007) 071913.
[14] D.S.L Abergel, A. Russell, V.I. Fal'ko, Appl. Phys. Lett. 91 (2007) 063125.
[15] R.P. Vidano, D.B. Fischbach, L.J. Willis, T.M. Loehr, Solid State Commun. 39 (1981) 341.
[16] C. Thomsen, S. Reich, Phys. Rev. Lett. 85 (2000) 5214.
[17] S. Han, X. Liu, C. Zhou, J. Amer. Chem. Soc. 127 (2005) 5294.
[18] P.H. Tan, Y.M. Deng, Q. Zhao, Appl. Phys. Lett. 74 (1999) 1818.
[19] I. Calizo, A.A. Balandin, W. Bao, F. Miao, C.N. Lau, Nano Lett. 7 (2007) 2645.
[20] N. Mounet, N. Marzari, Phys. Rev. B 71 (2005) 205214.
[21] N. Bonini, M. Lazzeri, N. Marzari, F. Mauri, Phys. Rev. Lett. 99 (2007) 176802.
[22] F. Parvizi, D. Teweldebrhan, S. Ghosh, I. Calizo, A.A. Balandin, H. Zhu, R. Abbaschian, Micro Nano Lett. 3 (2008) 29.
[23] A.A. Balandin, S. Ghosh, W. Bao, I. Calizo, D. Teweldebrhan, F. Miao, C.N. Lau, Nano Lett. 8 (2008) 902.
[24] S. Ghosh, I. Calizo, D. Teweldebrhan, E.P. Pokatilov, D.L. Nika, A.A. Balandin, W. Bao, F. Miao, C.N. Lau, Appl. Phys. Lett. 92 (2008) 151911.
[25] A.A. Balandin, Thermal conduction in graphene and graphene multilayers, Invited talk, in: International Symposium on Graphene Devices, Aizu-Wakamatsu, Japan, 2008.
[26] Q. Shao, G. Liu, D. Teweldebrhan, A.A. Balandin, Appl. Phys. Lett. 92 (2008) 202108.